The centriolar satellite protein Cep131 is important for genome stability

Christopher J. Staples[1], Katie N. Myers[1], Ryan D. D. Beveridge[1], Abhijit A. Patil[1], Alvin J. X. Lee[2], Charles Swanton[2], Michael Howell[3], Simon J. Boulton[4] and Spencer J. Collis[1,*]

[1]Genome Stability Group, CR-UK/YCR Sheffield Cancer Research Centre, YCR Institute for Cancer Studies, Department of Oncology, University of Sheffield Medical School, Beech Hill Road, Sheffield S10 2RX, UK
[2]High Throughput Screening Facility, CR-UK London Research Institute, 44 Lincoln's Inn Fields London WC2A 3LY, UK
[3]Translational Cancer Therapeutics Laboratory, Cancer Research UK London Research Institute, 44 Lincoln's Inn Fields, London WC2A 3LY, UK
[4]DNA CR-UK Damage Response Laboratory, London Research Institute, Clare Hall Laboratories, South Mimms EN6 3LD, UK
*Author for correspondence (s.collis@sheffield.ac.uk)

Accepted 6 June 2012
Journal of Cell Science 125, 4770–4779

doi: 10.1242/jcs.104059

Summary

The centrosome acts as a centre for microtubule organisation and plays crucial roles in cell polarity, migration, growth and division. Cep131 has recently been described as a basal body component essential for cilium formation, but its function in non-ciliogenic cells is unknown. We identified human Cep131 (also known as AZI1) in a screen for regulators of genome stability. We show that centrosomal localisation of Cep131 is cell-cycle-regulated and requires both an intact microtubule network and a functional dynein–dynactin transport system. Cep131 is recruited to centriolar satellites by PCM1, and localised to the centriolar core region by both pericentrin and Cep290. Depletion of Cep131 results in a reduction in proliferation rate, centriole amplification, an increased frequency of multipolar mitosis, chromosomal instability and an increase in post-mitotic DNA damage. These data therefore highlight the importance of human Cep131 for maintaining genomic integrity.

Key words: Centrosomal satellite proteins, Cep131, AZI1, Genome stability

Introduction

The centrosome is the primary site of microtubule nucleation and organisation during interphase and mitosis in diploid cells, and is important for cell growth, division, polarity and migration. It consists of two orthogonally positioned cylindrical centrioles surrounded by an electron-dense matrix of pericentriolar material (PCM) partly comprised of particles termed centriolar satellites. Microtubules are nucleated in the PCM from γ-tubulin ring complexes within a mesh-like structure that contains the protein pericentrin (Dictenberg et al., 1998; Gould and Borisy, 1977; Moritz et al., 1995). The formation of an organised microtubule array is in turn dependent on satellite proteins such as pericentriolar material 1 (PCM1), which is thought to act as a scaffold to recruit other proteins including pericentrin, ninein, Cep90 and Cep290 to the PCM (Dammermann and Merdes, 2002; Kim and Rhee, 2011; Lopes et al., 2011; Mogensen et al., 2000). This involves complex and incompletely characterised interactions between numerous satellite proteins and the dynein–dynactin microtubule minus end motor system (Dammermann and Merdes, 2002; Kim et al., 2008b; Kim et al., 2004; Kodani et al., 2010; Lee and Rhee, 2010).

Normally, the centrioles duplicate once per cell cycle, and this process is tightly linked to DNA replication (Balczon et al., 1995; Meraldi et al., 1999). The deregulation of centriole duplication and the subsequent formation of additional supernumerary centrosomes are associated with genetic instability and cancer development/progression (Emdad et al., 2005; Fukasawa, 2007; Nigg, 2006). The importance of an intact centrosome network is further highlighted by the finding that mutations in some centrosome proteins result in microcephaly and primordial dwarfism, while mutations in others affect cilia formation contributing to various ciliopathies (Nigg and Raff, 2009). However, the regulation of the human centrosome and its diverse cellular functions are complex and not fully understood. This is in part due to the fact that the human centrosome contains hundreds of proteins, many of which are poorly characterised (Andersen et al., 2003).

Cep131 (also termed azacytidine-inducible-1, AZI1) was initially discovered as a protein localised to the pre-acrosome region of the murine spermatid (Aoto et al., 1997; Aoto et al., 1995), and later identified in a large-scale proteomic screen for novel centrosomal proteins (Andersen et al., 2003). Little is known about Cep131's cellular function, although Zebrafish and Drosophila lacking Cep131 orthologues have shortened cilia, and display phenotypes reminiscent of human ciliopathies such as Bardet–Biedl syndrome (Ma and Jarman, 2011; Wilkinson et al., 2009). Interestingly, Cep131 depletion results in reduced ciliogenesis in human epithelial cells, with those cilia that do form exhibiting gross morphological defects (Graser et al., 2007). Cep131 is therefore a candidate for presently uncharacterised human ciliopathies. However, the function of Cep131 outside of ciliogenesis is currently unknown.

We have identified Cep131 in a human genome-wide siRNA-based screen as a candidate regulator of genome stability. In this paper, we characterise human Cep131 in non-ciliogenic cells and demonstrate that it is a component of centriolar satellites required for normal proliferation. Depletion of Cep131 results in centriole

Journal of Cell Science

amplification leading to an increased frequency of multipolar mitosis, chromosomal instability and post-mitotic DNA damage.

Results

Cep131 localisation is cell cycle regulated, and requires an intact microtubule network and active dynein–dynactin transport system

We recently carried out a siRNA-based screen for regulators of genome stability, using the fluorescent detection of H2AX phosphorylation on serine 139 (γH2AX) as an early marker of DNA damage (Bonner et al., 2008). A prominent candidate identified was Cep131; a protein until now recognised largely for its role in cilia formation (Graser et al., 2007; Ma and Jarman, 2011; Wilkinson et al., 2009). However, little else is known about the function of Cep131, especially in non-ciliogenic cells. In support of our findings, an independent screen confirmed that Cep131 depletion leads to increased H2AX phosphorylation (Paulsen et al., 2009). To validate the findings from our screen, we depleted Cep131 in additional cell lineages using four individual siRNA oligonucleotides that comprised the initial pool, and assessed γH2AX foci by immunofluorescence. Cep131 depletion was confirmed by western blotting (supplementary material Fig. S1A) and knockdown of Cep131 with all four siRNAs resulted in increased levels of γH2AX (supplementary material Fig. S1B).

Although Cep131 has been reported to localise to centrosomes (Andersen et al., 2003), the localisation of endogenous Cep131 in non-ciliogenic cells has not been studied in detail, nor have the factors responsible for its centrosomal localisation been determined. We therefore performed immunofluorescence for endogenous Cep131, observing that the majority of Cep131 localised to both the core centriolar region and centriolar satellites in interphase cells (Fig. 1A). Interestingly, Cep131 localisation exhibited a dynamic cell-cycle-dependent distribution; becoming markedly more concentrated at the centrosome just prior to mitosis. Cep131 centrosomal localisation was completely lost as

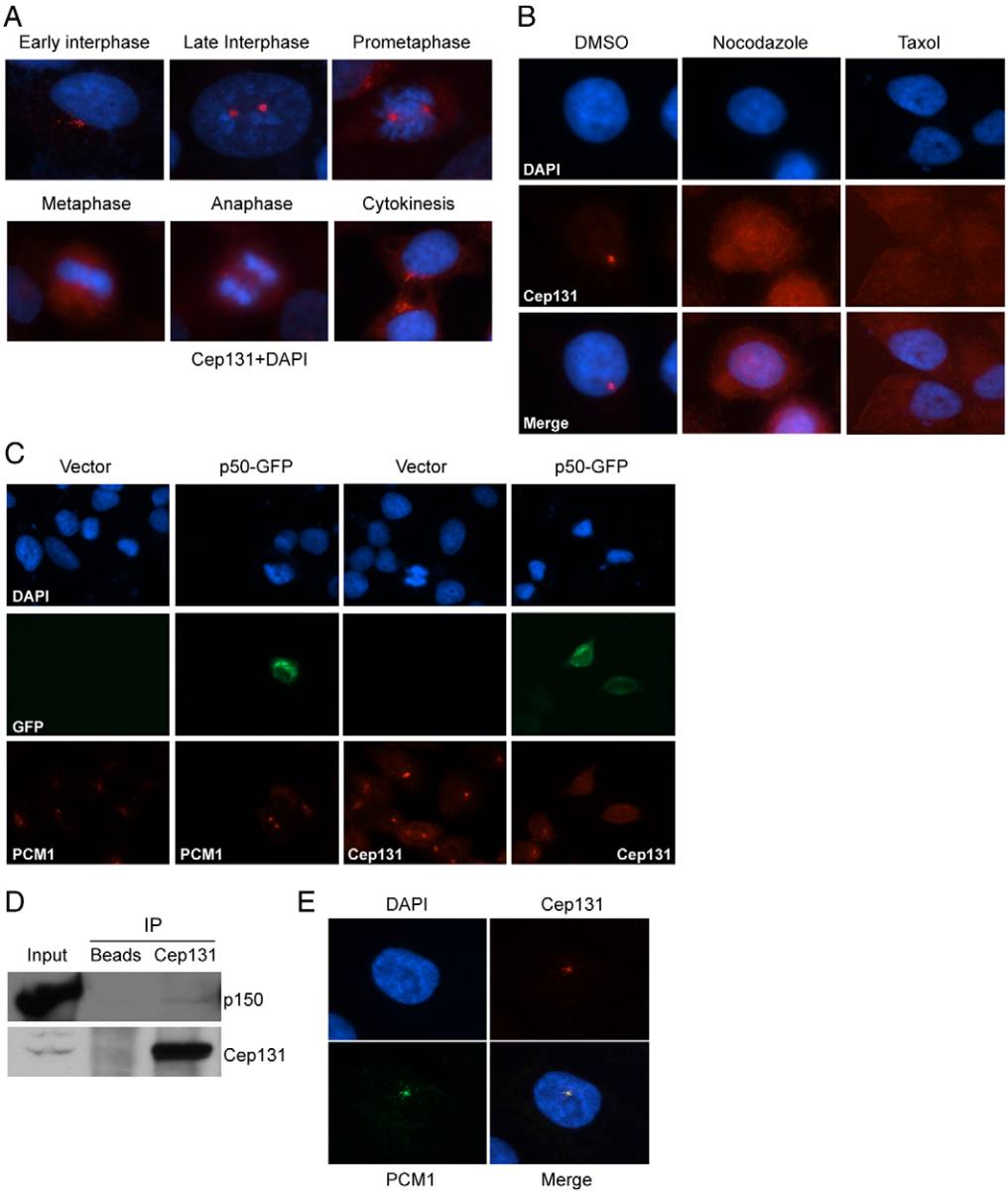

Fig. 1. Cep131 centrosomal localisation is dependent on cell cycle phase, microtubules and an intact dynein motor system. (**A**) Cells were fixed and stained for Cep131, and nuclei counterstained with DAPI. Cep131 localisation is represented in cells at various stages of the cell cycle as indicated. (**B**) Cells were treated with DMSO, 1 μg/ml nocodazole or 10 μM taxol for 3 hrs before fixation and staining for Cep131. (**C**) Cells were transfected with empty vector or a vector expressing GFP-tagged p50-dynamitin. After 24 hrs cells were fixed and stained for Cep131 or PCM1 as indicated. (**D**) Cep131 was immunoprecipitated from cell lysates using a rabbit anti-Cep131 antibody. Co-immunoprecipitated p150-glued was detected using a mouse anti-p150-glued antibody. The small fraction of p150-glued which co-immunoprecipitates with Cep131 probably reflects the transient nature of such an interaction. (**E**) Cells were fixed and stained for Cep131 and PCM1, and counterstained with DAPI to observe colocalisation. All experiments were performed at least three times and representative images are shown.

chromosomes aligned during metaphase, reforming once again during the latter stages of cytokinesis (Fig. 1A). The loss of Cep131 from centrosomes during mitosis was not associated with altered Cep131 protein levels, as total Cep131 levels assessed by western blot were unaffected in cells synchronised with nocodazole and released into mitosis (data not shown).

This localisation pattern is reminiscent of the centriolar satellite protein PCM1, which is known to redistribute during mitosis (Balczon et al., 1994). PCM1 localisation is dependent on the presence of intact microtubules and a functional dynein–dynactin transport system (Dammermann and Merdes, 2002). To investigate whether a similar mechanism might underlie Cep131 recruitment to centrosomes, we disrupted microtubules using either the microtubule depolymerising agent nocodazole or the microtubule stabilising agent taxol. Both treatments caused the complete disruption of the centrosomal localisation of Cep131 (Fig. 1B), suggesting that a dynamic microtubule network is required for the maintenance of Cep131 localisation. Compellingly, Cep131 was also mislocalised in cells in which the dynein–dynactin system was disrupted by the overexpression of p50-dynamitin (Fig. 1C), highlighting a potential role for this transport system in the localisation of Cep131. In agreement with this finding, we observed an interaction between endogenous Cep131 and the dynactin subunit p150-glued (Fig. 1D), and co-localisation between Cep131 and PCM1 (Fig. 1E).

PCM1 and pericentrin are respectively required for the pericentriolar satellite and centriolar localisation of Cep131

We next sought to determine if PCM1 is required for Cep131 localisation. PCM1 was depleted in a HeLa cell line stably expressing GFP-tagged centrin-2 (a centriole marker) and localisation of endogenous Cep131 was assessed by immunofluorescence. Identical experiments were also performed in U2OS osteosarcoma cells. PCM1 depletion resulted in the loss of Cep131 from pericentriolar satellites, although Cep131 localisation at the centriolar core was unaffected (Fig. 2A; supplementary material Fig. S2A). This is interesting in the light of our earlier finding that Cep131 was completely mislocalised from both centrosomal regions by nocodazole and taxol treatments, as well as p50-dynamitin overexpression. This suggests that additional, microtubule-dependent but PCM1-independent mechanisms exist to recruit Cep131 to the centriolar region. Since pericentrin is known to be a dynein cargo protein (Tynan et al., 2000; Young et al., 2000) and interacts with PCM1 (Li et al., 2001), we hypothesised that pericentrin may be required to recruit Cep131 to the centriolar core region. We therefore depleted pericentrin in both GFP–centrin-expressing HeLa cells and U2OS cells and examined the localisation of PCM1 and Cep131 by immunofluorescence. Pericentrin depletion resulted in the complete mislocalisation of both Cep131 and PCM1 (Fig. 2A,B; supplementary material Fig. S2A). The effect on PCM1 is in keeping with the observation that pericentrin is required for the localisation of DISC1, a centrosomal protein that contributes to PCM1 localisation (Kamiya et al., 2008; Miyoshi et al., 2004). Cep131 and PCM1 may therefore require pericentrin in order to act as cargo for dynein/dynactin molecular motors.

PCM1 is thought to assist in maintaining the centrosomal localisation of pericentrin via a mechanism involving dynein–dynactin-mediated transport (Dammermann and Merdes, 2002), although a significant proportion of cellular pericentrin localises to the centrosome independently of this mechanism via a

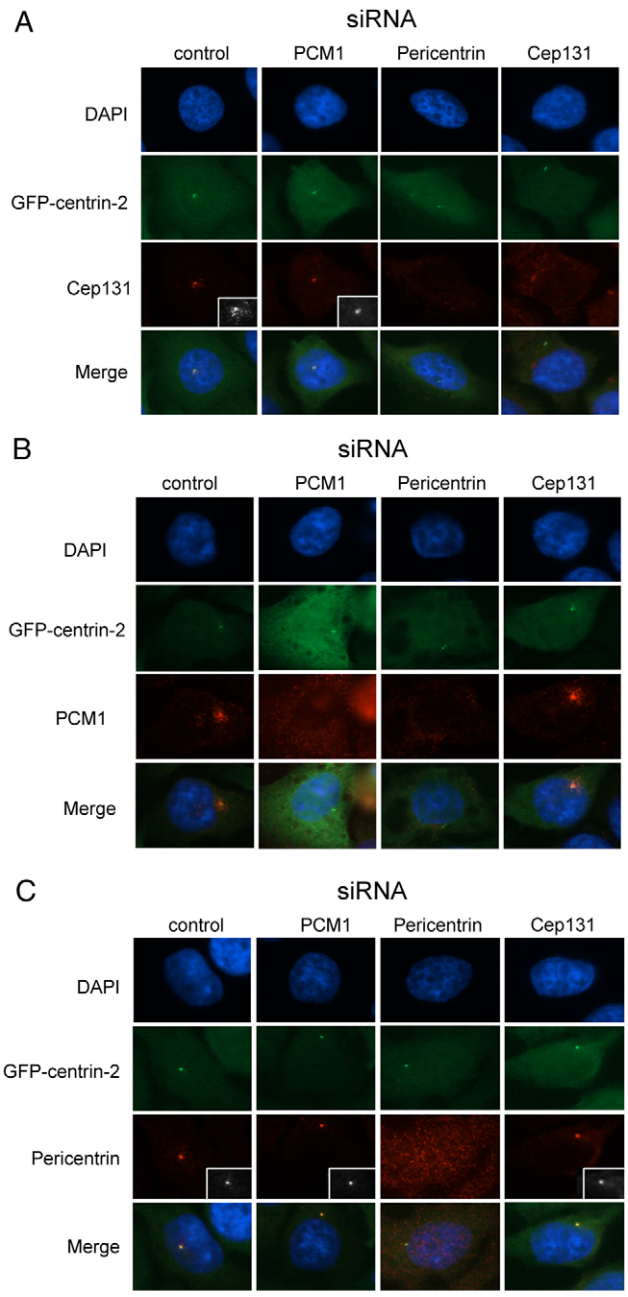

Fig. 2. Cep131 is recruited to the pericentriolar satellite and centriolar core regions in a PCM1- and pericentrin-dependent manner. HeLa cells stably expressing GFP-tagged centrin-2 were transfected with non-targeting control siRNA, or siRNAs targeting PCM1, pericentrin or Cep131 as indicated. After 48 hrs cells were fixed, stained for (**A**) Cep131, (**B**) PCM1, or (**C**) pericentrin and counterstained with DAPI. Boxes in the lower right of figures show a magnification of the centrosome to highlight subtle differences in satellite localisation. All experiments were performed at least three times and representative images are shown.

C-terminal PACT domain (Gillingham and Munro, 2000). In agreement with these reports, we observed a decrease in pericentrin satellite localisation following PCM1 depletion (Fig. 2C). Recent work by others has shown that the localisation of a number of centrosomal proteins involved in ciliopathies including PCM1, BBS4, OFD1 and Cep290, is

mutually inter-dependent (Lopes et al., 2011). This phenomenon may reflect a mutual requirement between these proteins for efficient loading to the dynein motor complex. With this in mind, we assessed the effect of Cep131 depletion on the centrosomal localisation of PCM1 and pericentrin. However, neither PCM1 (Fig. 2B) nor pericentrin (Fig. 2C) localisation were significantly altered by Cep131 depletion, suggesting that Cep131 does not mediate interactions between the dynein motor and its satellite protein cargoes, and as such is not essential for satellite integrity.

Cep131 interacts with PCM1, pericentrin and Cep290

Given that Cep131 localisation to pericentriolar and centriolar core regions is dependent on PCM1 and pericentrin respectively, we performed immunoprecipitation experiments to confirm whether Cep131 interacts with PCM1 and/or pericentrin. Both endogenous PCM1 and pericentrin reciprocally co-purified with endogenous Cep131 (Fig. 3A,B). We noted that PCM1 and pericentrin which co-purified with Cep131 exhibited reduced electrophoretic mobility after SDS-PAGE, compared to input lanes (Fig. 3B). To confirm that these retarded proteins corresponded to endogenous PCM1 and pericentrin, we employed appropriate siRNA as indicated in Fig. 3A. The ability of Cep131 and pericentrin to interact in PCM1-depleted cells is consistent with our finding that PCM1 is not required for the centriolar localisation of Cep131 (Fig. 2A). It is interesting to note that we consistently observed that Cep131 and PCM1 interacted in pericentrin-depleted cells (Fig. 3A). This suggests that Cep131 and PCM1 can form a complex in the absence of pericentrin, although this complex appears not to be transported to centriolar satellites (Fig. 2A,B).

A mutual requirement exists between PCM1 and several ciliopathy-associated proteins for centriolar localisation (Lopes et al., 2011) including Cep290, which is mutated in a range of ciliopathies (Coppieters et al., 2010) and has recently been shown to interact with PCM1 (Kim et al., 2008b). We therefore hypothesised that Cep131 might also interact with Cep290 to promote its localisation. Consistently, we were able to reciprocally co-immunoprecipitate endogenous Cep290 and Cep131 (Fig. 3C). Given this finding, we examined whether Cep131 was required for the centrosomal localisation of Cep290. However, unlike PCM1 and pericentrin, Cep131 depletion had no effect on the centrosomal localisation of Cep290 (supplementary material Fig. S2B). Interestingly, BBS4, which is also known to bind PCM1 and assist in maintaining its localisation (Kim et al., 2004), was not recovered in Cep131 immunoprecipitates (data not shown). This suggests that the interaction between Cep131 and Cep290 might be functionally important, and also lends support to the idea that functionally and compositionally distinct PCM1-containing protein complexes exist within centriolar satellites.

Given these findings, we next depleted cells of Cep290 to determine whether Cep290 is required for Cep131 centrosomal localisation. Cep290 depletion resulted in the mislocalisation of Cep131 from both the pericentriolar satellite and centriolar core regions (Fig. 3D). This was not a result of mislocalisation of pericentrin (Fig. 3D), even though Cep290 and pericentrin co-purify (Fig. 3E), and Cep290 pericentriolar satellite localisation is partially dependent on pericentrin (supplementary material Fig. S2B). In agreement with recent findings (Lopes et al., 2011), PCM1 was also mislocalised following Cep290 depletion (Fig. 3D). This may account for a proportion of Cep131 not recruited to pericentriolar satellites; however, the additional loss of Cep131 from the centriolar core region suggests that Cep290 and pericentrin-dependent mechanisms also exist to recruit Cep131 to the centriolar region independently of PCM1. Overall, these data confirm Cep131 as a component of

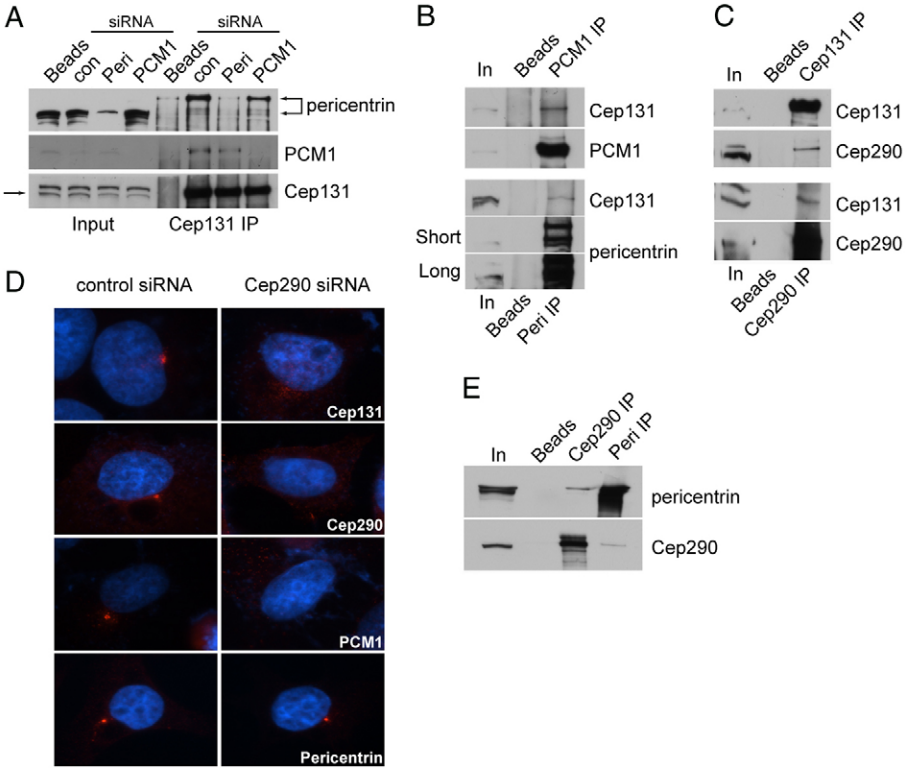

Fig. 3. Cep131 interacts with PCM1, pericentrin and Cep290. (**A**–**C**) Endogenous Cep131, PCM1, pericentrin or Cep290, as indicated, were immunoprecipitated (IP) from HEK293 whole-cell lysates. Immunoprecipitates were probed with the indicated antibodies. In panel A, cells were treated for 48 hrs with the indicated siRNA prior to IP. Short and long exposures are shown in panel C to highlight efficient pericentrin immunoprecipitation. In, input, and arrows highlight Cep131 and pericentrin bands. (**D**) Cells were transfected with either a control or Cep290 targeting siRNA. After 48 hrs, cells were fixed, stained for Cep131, Cep290 or PCM1 and counterstained with DAPI. (**E**) Endogenous Cep290 and pericentrin were immunoprecipitated from HEK293 whole-cell lysates and probed with the indicated antibodies. All experiments were performed three times and representative images are shown.

pericentriolar satellites, prove an endogenous interaction between Cep131 and PCM1, pericentrin and Cep290, and demonstrate that while Cep131 clearly has an important role in cilia formation and is recruited by centriolar satellite proteins, it does not appear to be required for the maintenance of satellite integrity in non-ciliogenic cells.

Cep131 is not required for microtubule organisation, but is required for efficient proliferation

Depletion of centrosomal proteins such as PCM1 causes defects in interphase microtubule organisation, whilst the depletion of pericentrin interferes with microtubule nucleation (Dammermann and Merdes, 2002; Dictenberg et al., 1998). To determine whether Cep131 affects microtubules, we depleted U2OS cells of Cep131 and assessed microtubule organisation by staining fixed cells with an antibody against α-tubulin. U2OS cells have previously been exploited due to their well-organised radial interphase microtubule array (Dammermann and Merdes, 2002). U2OS cells were co-stained with either Cep131 to confirm effective knockdown, or pericentrin to mark the centrosome. As a positive control, cells were also depleted of PCM1. In agreement with the findings of Dammermann and Merdes, we found that PCM1 depletion resulted in a marked loss of radial microtubule organisation (supplementary material Fig. S3A,B). However, despite effective depletion of Cep131, we did not observe any such defect in microtubule organisation (supplementary material Fig. S3A,B), suggesting that Cep131 does not play a role in the promotion of microtubule organisation by PCM1.

Centrosomal proteins including pericentrin are also important for cancer cell growth (Kim et al., 2008a). To investigate whether Cep131 plays a similar role in regulating cell growth, we depleted Cep131 using two independent siRNAs and assessed cell cycle profiles using flow cytometry following propidium iodide staining. In agreement with previous observations (Graser et al., 2007), Cep131 depletion did not result in any gross alterations in cell cycle phase (Fig. 4A). However, we consistently observed a significant decrease in replicating cells following Cep131 depletion (Fig. 4B), which was accompanied by a significant decrease in the proportion of mitotic cells (Fig. 4C). Interestingly, live cell imaging of HeLa cells stably expressing GFP-tagged histone H2B revealed no significant defect in the kinetics of mitosis following Cep131 depletion (Fig. 4D). However, Cep131-depleted cells grew significantly more slowly than cells transfected with non-targeting control siRNAs (Fig. 4E). This growth defect was similar in magnitude to that observed when PCM1 levels were depleted, but was much less severe than the growth defect observed following pericentrin depletion (data not shown). Together, these results indicate that Cep131 is necessary for optimal cell proliferation.

Cep131 depletion results in centrosome duplication defects and genomic instability

Centrosome amplification has long been associated with cancer, and more recently with chromosomal instability and mis-segregation (Ganem et al., 2009; Silkworth et al., 2009). To investigate the possibility that Cep131 is important for efficient duplication, we depleted Cep131 using two independent siRNAs and stained cells for pericentrin, which remains at the spindle pole during mitosis. Cep131 depletion resulted in an increased proportion of mitotic cells with multi-polar spindles, which we observed in multiple cell lineages (Fig. 5A and data not shown). We also observed an increased frequency of pseudo-bipolar spindles in Cep131-depleted cells, which are presently thought to represent a mechanism by which cancer cells reduce spindle multi-polarity by promoting the clustering of additional centrosomes on a bipolar axis (Krämer et al., 2011; Silkworth et al., 2009). Analysis of GFP–centrin-2-expressing cells revealed that Cep131 depletion resulted in an increase in the proportion of cells with additional GFP–centrin-2 structures (Fig. 5B,C). To determine whether these centrin foci might represent additional centrioles, we stained Cep131-depleted GFP–centrin-2-expressing HeLa cells for the centriolar linker protein C-Nap1, which is localised to the proximal end of the centrioles. The majority of additional centrin structures in Cep131-depleted cells did not stain for C-Nap1, but did stain the pericentriolar material and partially co-localised with PCM1, suggesting that these represent centriolar satellites (Fig. 5B,C). However, a significant sub-fraction of cells (12–15%) contained extra centrin structures that also co-stained with C-Nap1 (Fig. 5B). These structures therefore likely represent bona fide additional centrioles and highlight a supernumerary centrosomes phenotype in Cep131-deficient cells.

We also found that Cep131-depleted cells display an increased frequency of nuclear abnormalities including micronuclei and chromatin bridges (Fig. 6A) indicating an increased frequency of chromosome segregation errors. In agreement with these observations and recent data from other groups (Janssen et al., 2011), phosphorylation of the DNA damage checkpoint kinases ATM and Chk2 were also increased in cells depleted of Cep131 (Fig. 6B and Fig. 6C, respectively). These data suggest that mitotic chromosome segregation errors occur in the absence of Cep131, leading to the generation of DNA breaks and activation of the DNA damage response. To investigate this further, we performed cell cycle block-and-release experiments using the iron chelator mimosine. Mimosine was chosen because it causes arrest in G1 without centrosome over-duplication (Prosser et al., 2009). Treatment with mimosine prevented the increase in γH2AX observed following Cep131 depletion, suggesting that cell cycle progression is required for DNA damage to occur (Fig. 6D). Interestingly, increased γH2AX was only observed in Cep131-depleted cells released from a mimosine block after they were allowed to pass through mitosis (Fig. 6D). These data support a model where depletion of Cep131 leads to mitotic progression with centriole amplification/supernumerary centrosomes, giving rise to chromosomal aberrations and the generation of DNA damage.

Discussion

We have characterised human Cep131 as a component of centriolar satellites in non-ciliogenic cells, and demonstrate that Cep131 is important for cell proliferation, efficient centrosome duplication and facilitates genome stability.

We show that Cep131 localises to the centrosome in a cell-cycle-dependent manner and is also dependent on the presence of an intact microtubule network and a functional dynein–dynactin transport system. Cep131 localisation to pericentriolar satellites is dependent on PCM1, while localisation to the centriolar core is dependent on both pericentrin and Cep290. These data are in agreement with previous observations that centriolar satellites are not detected around the centrioles in dividing cells (Balczon et al., 1994), and that the localisation of PCM1 and pericentrin are also dependent on dynein–dynactin-mediated transport (Kim et al., 2004; Tynan et al., 2000; Young et al., 2000). Our finding that the pericentriolar satellite localisation of Cep131 is dependent on

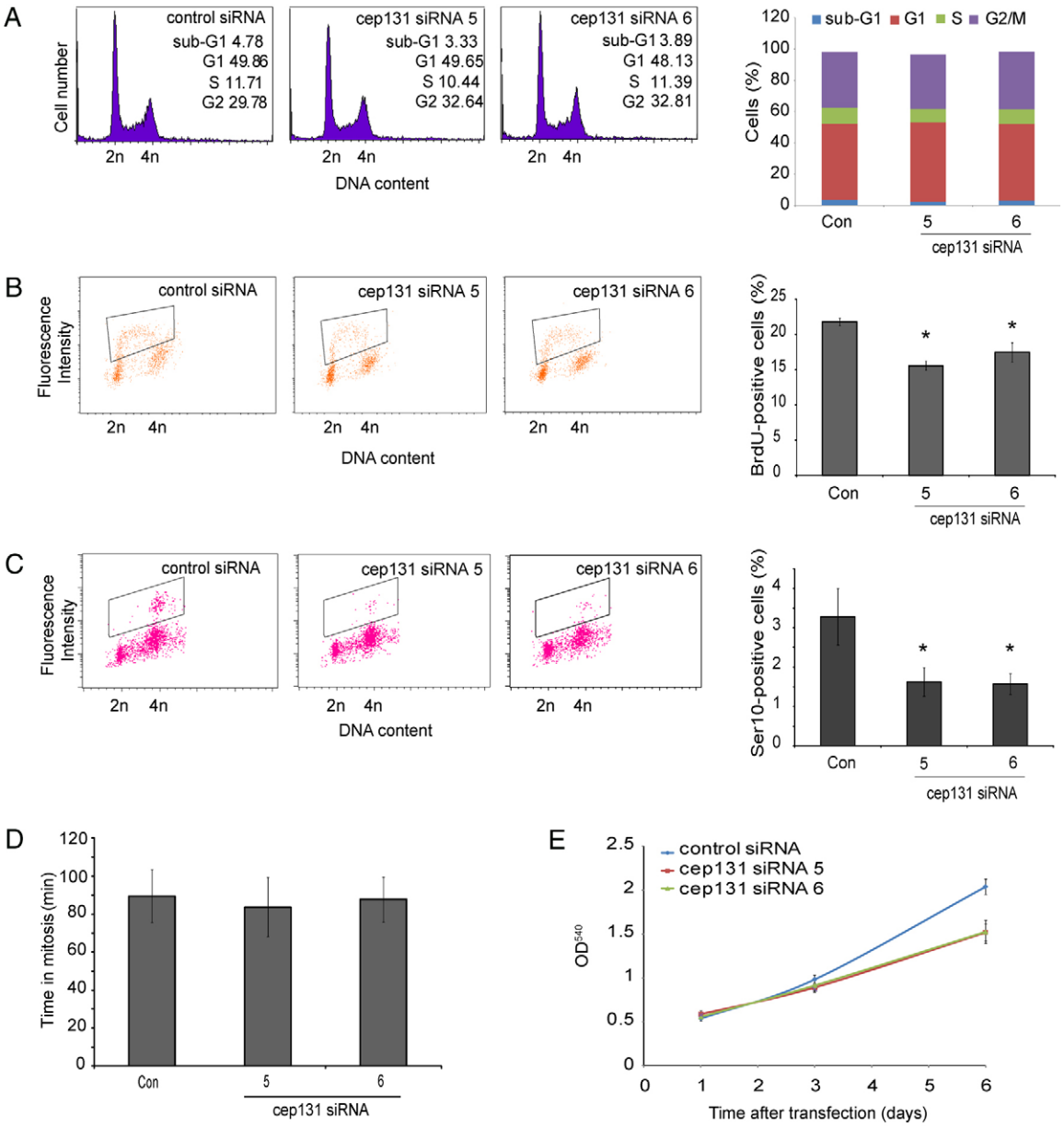

Fig. 4. Cep131 promotes proliferation and cell cycle progression. (**A**) Cells were transfected with a control siRNA, or two different individual siRNAs targeting Cep131. After 48 hrs, cells were fixed in ethanol and stained with propidium iodide. The experiment was performed three times in triplicate. Cell cycle phase was quantified and is shown on the right. The cell cycle phase of Cep131-depleted cells was not significantly different from cells transfected with control siRNA ($P>0.05$, Student's *t*-test). (**B**) Cells were transfected as in A, and after 48 hrs, cells were pulsed with BrdU for 20 min, then fixed in ethanol and stained for BrdU and propidium iodide to visualise actively replicating cells. (**C**) Cells were transfected as in A, and after 48 hrs, cells were fixed in ethanol and stained for histone H3 phosphorylated on serine 10 (an early mitotic marker) and with propidium iodide. Experiments were performed three times in duplicate. (**D**) HeLa cells stably expressing GFP-tagged histone H2B were transfected as in A, and after 48 hrs, live cells were followed for a period of 8 hrs by time-lapse microscopy. The duration of mitosis was determined from chromatin condensation to cytokinesis. Results shown represent the means±s.e.m. (**E**) Cells were plated at low density, transfected as in A, and after 1, 3 and 6 days, proliferation was assessed using the MTT assay. The experiment was performed three times in at least quadruplicate. Results shown are means±s.e.m. *$P<0.05$ (Student's *t*-test).

PCM1 supports a growing body of evidence suggesting that PCM1 recruits proteins involved in human ciliopathies to satellites via the dynein–dynactin motor system, including BBS4, Cep290 and OFD1 (Dammermann and Merdes, 2002; Kodani et al., 2010; Lopes et al., 2011). In contrast, Cep131 is unique amongst centrosomal satellites, as depletion does not affect the localisation of PCM1, pericentrin or Cep290.

The co-dependence between satellite proteins for localisation recently highlighted by Lopes and colleagues (Lopes et al., 2011) makes it difficult to define specific roles for individual satellite proteins in these intriguing structures. However, our finding that both pericentrin and Cep290 are required for the localisation of Cep131 to both pericentriolar satellite and centriolar core regions suggests that although dispersal of Cep131 from pericentriolar

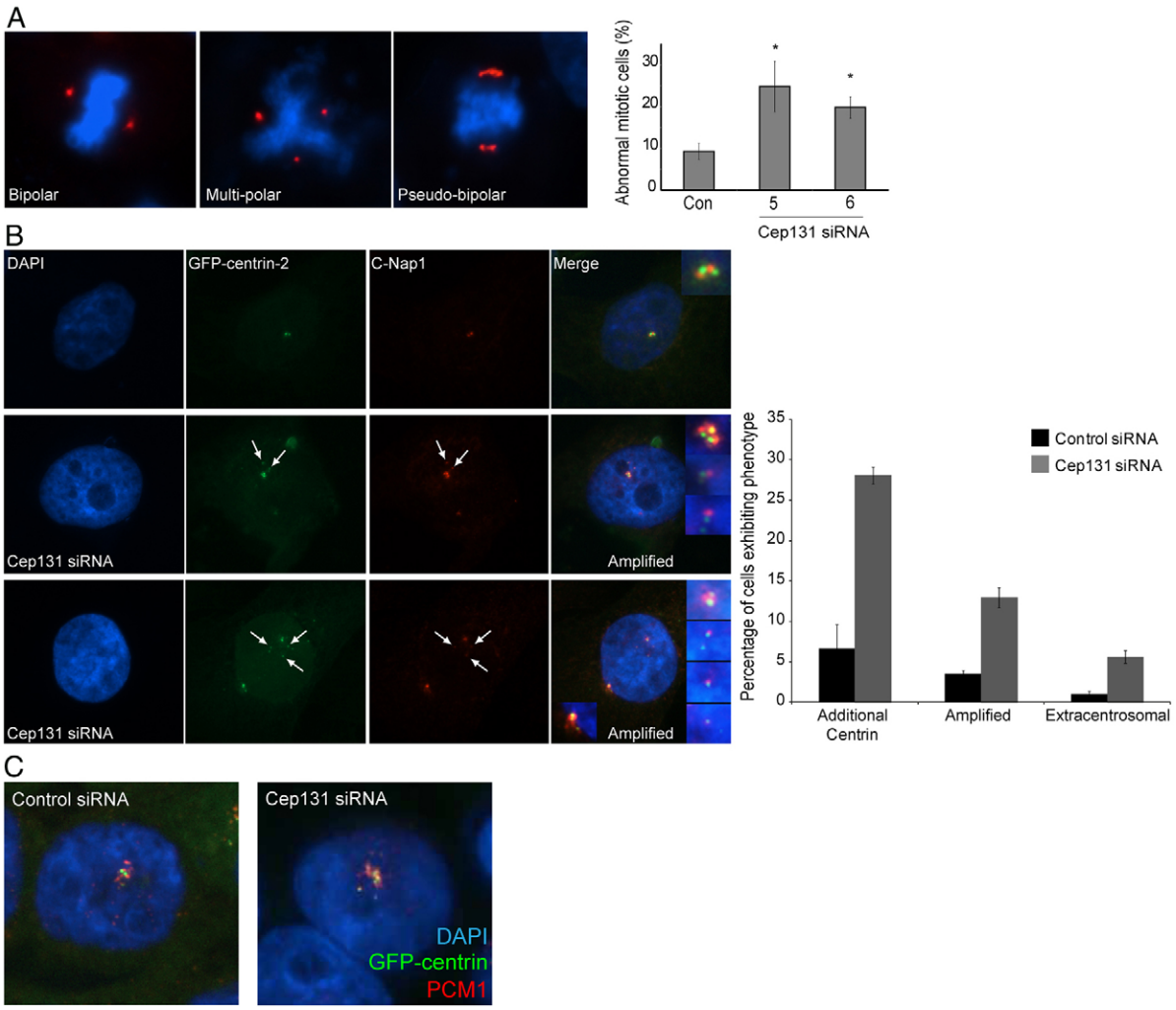

Fig. 5. Centrosome amplification defects are increased in Cep131-depleted cells. (**A**) HeLa cells were transfected with control or Cep131 siRNA, as described in Fig. 4A, then fixed and stained for pericentrin to mark the location of centrosomes. Nuclei were counterstained with DAPI. Representative examples of normal bipolar, multipolar and pseudo-bipolar mitoses are shown (left panels). Over 50 mitotic cells per experiment were assessed for the presence of multipolar or pseudo-bipolar spindles, and quantified for each siRNA treatment (right panel). (**B**) HeLa cells expressing GFP-tagged centrin-2 were transfected with control or Cep131 siRNA. After 24 hrs, cells were treated with 300 μM mimosine for 24 hrs, and then released into normal medium for 16 hrs before fixation to create a G1-enriched population. Cells were stained for C-Nap1 and the nuclei counterstained with DAPI. Over 200 cells per transfection were assessed for the presence of additional GFP–centrin-2 structures and C-Nap1 staining. Examples of normal and amplified GFP-centrin-2 and C-Nap1-positive structures are shown in the left panels. Centriole amplification was scored by the presence of >2 C-Nap1 and >4 centrin foci ('amplified'). A sub-fraction of these cells also contained additional extracentrosomal C-Nap1-positive GFP-centrin 2 foci ('extracentrosomal'), which are shown on the graph in the right panel. Results shown represent the mean (±s.e.m.) of two independently performed experiments. *$P<0.05$ (Student's *t*-test). (**C**) GFP–centrin-2-expressing HeLa cells were transfected with control siRNA or an siRNA targeting Cep131, and stained for PCM1.

satellites in Cep290-depleted and pericentrin-depleted cells may be a consequence of PCM1 mislocalisation (Kim et al., 2008b), Cep290 and pericentrin-dependent mechanisms also exist to recruit Cep131 to the centriolar core region independently of PCM1. It is interesting to note the phenotypic pleiotropy associated with the wide range of Cep290 mutations (Coppieters et al., 2010), and we hypothesise that these may result in part from a similarly broad range of effects on local protein–protein interactions associated with Cep290. As such, certain mutant alleles of Cep290 might result in satellite dispersal via loss of PCM1 localisation, while others may affect the localisation of specific proteins such as Cep131.

To our knowledge, the role of pericentrin in maintaining the localisation of pericentriolar satellite proteins has not previously been examined in detail. We demonstrate that pericentrin is required for the correct localisation of PCM1, Cep290 and Cep131, suggesting that pericentrin plays a previously unappreciated and critical role in satellite integrity. PCM1 is recruited to centrosomes in part via the dynein–dynactin motor system (Dammermann and Merdes, 2002; Kim et al., 2004), and pericentrin is known to interact with, and be recruited to the centrosome, by interaction with the dynein light intermediate chain (Tynan et al., 2000; Young et al., 2000). PCM1 and Cep131 may thus require pericentrin in order to act as cargo for dynein/

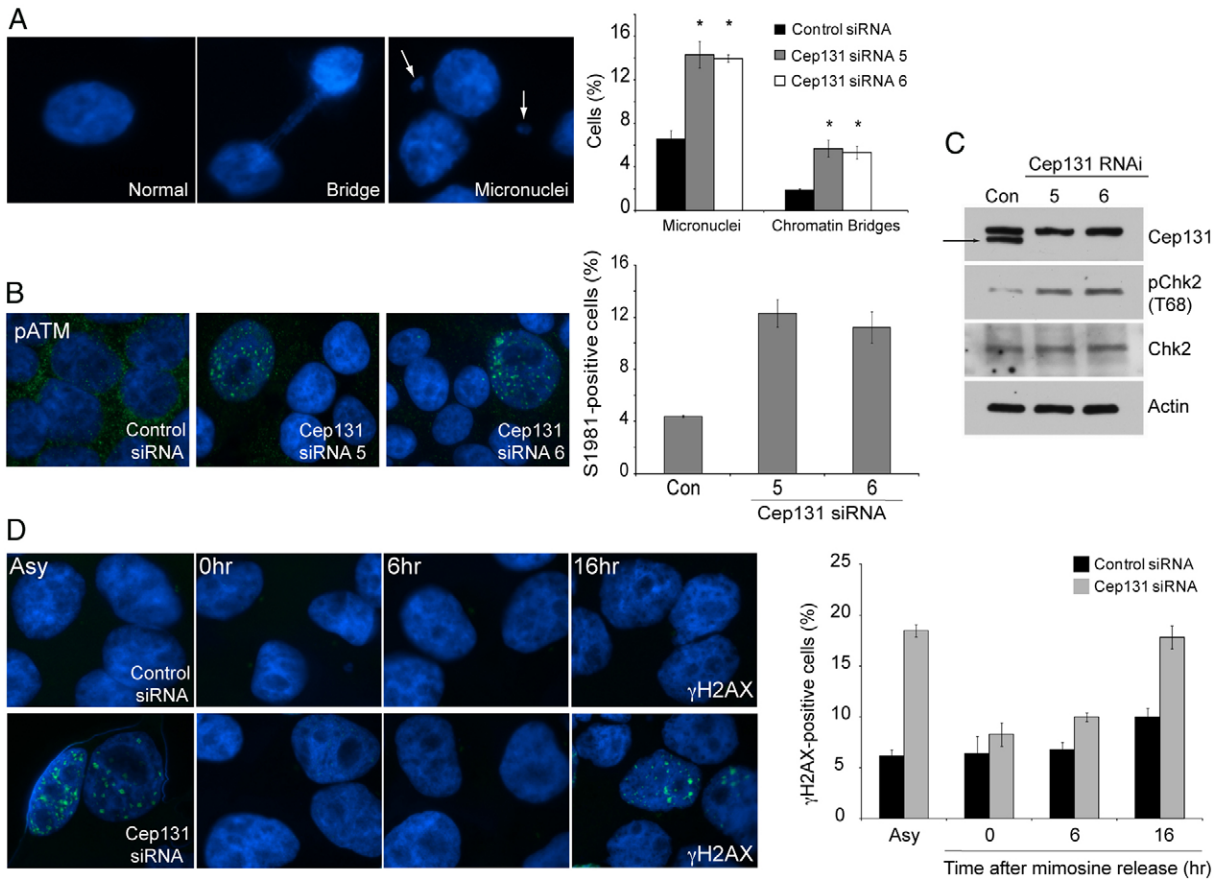

Fig. 6. Cep131-depletion results in chromosome segregation defects, and activates the DNA damage response. (**A**) Cells were transfected with a control siRNA, or two different individual siRNAs targeting Cep131. After 48 hrs, cells were fixed and stained with DAPI. Cells were assessed for the presence of micronuclei and chromatin bridges as highlighted (arrows). (**B**) Cells were siRNA-transfected and fixed as in A, stained for phosphorylated ATM (pATM, on Ser1981), and counterstained with DAPI. Representative examples of staining are shown in the left panels, and a quantification of pSer1981-positive cells from three independent experiments (>200 cells scored per experiment) is shown in the right panel. (**C**) Cells were treated with siRNA as in A, then lysed, and whole cell extracts were analysed by western blotting using the indicated antibodies. (**D**) HeLa cells expressing GFP-tagged centrin-2 were transfected with control or Cep131 siRNA as described in Fig. 4A. After 24 hrs, cells were treated with 300 μM mimosine for 24 hrs, then released into normal medium for the indicated times. Confirmation of an efficient G1 block and subsequent cell cycle progression was determined by propidium iodide incorporation and FACS analyses of cells at appropriate time points (data not shown). At the indicated times post-release, cells were fixed, stained for γH2AX and the nuclei counterstained with DAPI (left panels). Over 200 cells per transfection were assessed for γH2AX staining and the percentage of positively staining cells was quantified following each siRNA treatment (right panel). Results shown represent the mean±s.e.m. of three independently performed experiments. *$P<0.01$ (Student's *t*-test).

dynactin molecular motors. We also observed that distinct, but not necessarily independent, mechanisms exist to recruit Cep131 to pericentriolar satellites and centriolar core regions. It is therefore possible that unidentified functions of pericentrin and PCM1 are executed at least in part via the recruitment of Cep131.

We consistently observed cells with additional centrin-2 foci following Cep131 depletion, with the majority of these structures residing within the pericentriolar material as evidenced by co-staining with PCM-1, indicating that they may in fact represent centriolar satellites. Consistent with this finding, a small but significant fraction of these structures stained for the centriole marker C-Nap1, suggesting that Cep131 is important for the composition and distribution of centrin-containing satellite granules. This is interesting given recent data implicating centrin-positive satellites and the dynein transport system in centriole overduplication in S-phase-arrested CHO cells (Prosser et al., 2009). However, it must be noted that we did not observe any difference in the amounts of nuclear centrin in Cep131-depleted cells exhibiting extra centrin structures (data not shown). Additionally, a recent study demonstrated that new centrioles could arise in an expanded PCM matrix formed by overexpressed pericentrin (Loncarek et al., 2008). We therefore hypothesise that the centrin-containing satellites in Cep131-depleted cells might therefore promote the formation of additional centrioles, albeit at a low frequency.

Given that we originally identified Cep131 in a screen for novel genome maintenance factors using γH2AX as a marker of increased DNA damage, it is interesting to note that Cep131 appears unique among centriolar satellite proteins in this role. Depletion of OFD1 or Cep290 had no effect on γH2AX formation, while PCM1 or pericentrin depletion actually decreased the proportion of cells with γH2AX foci (data not shown). This last observation is in agreement with findings in Seckel patients harbouring nonsense mutations in pericentrin (Griffith et al., 2008). Of considerable interest is our finding that Cep131 depletion results in an increased number of cells

undergoing multipolar mitosis, and we hypothesise that this may be responsible at least in part for the genome instability observed in Cep131-depleted cells. In support of this theory, we show that mitotic transit leads to increased levels of DNA damage in Cep131-depleted cells.

Centrosome amplification and multipolar mitoses are known to cause chromosome missegregation (Silkworth et al., 2009), and the observed increase in centrosome amplification, nuclear abnormalities, DNA damage, and ATM and Chk2 phosphorylation in Cep131-depleted cells are in keeping with the findings of a recent study demonstrating that mitotic chromosome segregation errors cause DNA breaks and activation of the DNA damage response (Janssen et al., 2011). Cep131 therefore joins an expanding group of human centrosomal proteins including Cep63, Cep164, Cep152 and pericentrin that are important for maintaining genome stability (Griffith et al., 2008; Kalay et al., 2011; Sivasubramaniam et al., 2008; Smith et al., 2009). It is interesting to note that several of these proteins are phosphorylated by the DDR kinases ATM and/or ATR, and a putative SQ phosphorylation motif is found in Cep131 (Matsuoka et al., 2007). We are currently assessing whether Cep131 is a substrate for these kinases and what biological effect any modification to this site has on Cep131 function.

Materials and Methods

Antibodies

Abcam; Cep131 (ab84864 for immunofluorescence and ab99379 for immunoprecipitation and western blotting), pericentrin (ab4448), Cep290 (ab85728), phospho-histone H3 Ser10 (ab14955) and β-actin (ab8224). Cell Signaling Technologies; γH2AX Ser139 (no. 2577), phospho-Chk2 (Ser68; no. 2661), Chk2 (no. 2662) and rabbit anti-PCM1 (Q-15, no. 5259). Abnova: mouse anti-PCM1 (4152-B01). BD Transduction Labs: mouse anti-p150-glued (612709). C-Nap1 was a kind gift from Professor Erich Nigg (University of Basle, Switzerland). For flow cytometric analysis of BrdU incorporation, mouse monoclonal anti-BrdU (DAKO clone BU20a) was used and this was visualised using rabbit anti-mouse FITC (DAKO, F0232). For western blotting, primary antibodies were visualised using HRP-conjugated secondary antibodies from DAKO. For immunofluorescence, Invitrogen anti-mouse Alexa Fluor 488 or anti-rabbit Alexa 545 were used.

Cell culture

HeLa, U2OS and HEK293 cells were maintained as an adherent monolayer in DMEM media containing 10% FBS and 1% penicillin/streptomycin at 37℃ in a humidified atmosphere of 5% carbon dioxide. HeLa Flp-in T-Rex and HEK293 Flp-In T-Rex cells (Invitrogen) were maintained in DMEM media containing 10% FBS and 1% penicillin/streptomycin, supplemented with 4 μg/ml Blasticidin S (Melford) and 100 μg/ml Zeocin (Invitrogen). HEK293 Flp-In cells were maintained in identical media supplemented with 100 μg/ml Zeocin (Invitrogen). HeLa cells stably expressing GFP-tagged Histone H2B were maintained in identical media supplemented with 2 μg/ml Blasticidin S. HeLa cells stably expressing GFP-tagged centrin-2 were maintained in identical media supplemented with 400 μg/ml G418 (Sigma).

Stable cell line generation

Stable tetracycline-inducible HEK293 Flp-In cell lines expressing FLAG-tagged Cep131 and HeLa Flp-In cell lines expressing YFP or FLAG-tagged Cep131 were created by co-transfection of these cell lines with pPGKFLPobpA-Flp recombinase and either empty pDEST-Flag/FRT/TO or pDEST-Flag/FRT/TO-Cep131 according to the Flp-In manufacturer's protocol. Recombinants were then selected in media containing 4 μg/ml Blasticidin S and 150 μg/ml Hygromycin B (Invitrogen). All transient transfections were performed using Lipofectamine 2000 (Invitrogen) according to the manufacturer's instructions.

Transfections and drug treatments

HEK293 and HeLa cells were transfected with 50 nM siRNA using Lipofectamine 2000 (Invitrogen) according to the manufacturer's instructions. Cells were collected, lysed or fixed for analysis after 48 hrs unless otherwise indicated. Cells were treated with 1 μM nocodazole (Sigma) or 10 μM Taxol (Sigma) for 3 hrs or 300 μM mimosine (Sigma) before fixation or release into drug-free medium for the times indicated.

Cell lysis and western blotting

For whole-cell extracts, the cells were solubilized on ice in lysis buffer (20 mM Tris-HCl pH 7.5, 150 mM NaCl, 1% Triton X-100, 1 mM DTT and 1 mM EDTA) supplemented with 50 U/μl benzonase (Novagen), protease and phosphatase inhibitors (Sigma). Cleared lysates were produced by centrifugation of the resulting samples at 16,000 ***g*** for 15 min at 4℃. Gel electrophoresis was performed using the NuPAGE system (Invitrogen). Briefly, samples were resolved on 4–12% Bis-Tris gels in MOPS buffer, transferred to a PVDF membrane which was then probed for the protein of interest using antibodies diluted in PBS containing 5% Marvel and 0.1% Tween-20 (Sigma).

Immunoprecipitation

For purification of FLAG-tagged proteins, 1 mg of the whole-cell extract was incubated with 20 μl of M2-anti FLAG beads (Sigma) for 16 hrs at 4℃. For immunoprecipitations using endogenous antibodies, 1–2 μg of antibody was incubated with the sample for 1–2 hrs before addition to 20 μl of washed Protein A/G beads (Santa Cruz) and incubation for 16 hrs at 4℃. Beads were then pelleted and washed three times in 20×bed volume of the lysis buffer. The bound protein was eluted either by heating the beads at 95℃ for 5 min with 2×LDS buffer (Invitrogen) or by incubation with FLAG peptide (Sigma) according to manufacturer's instructions. Inputs represent ~1/40th of the extract used for the immunoprecipitation.

Immunofluorescence and live-cell imaging

Cells were grown on glass coverslips and treated as indicated, then fixed with either methanol or 3% buffered paraformaldehyde for 10 min at RT, and permeabilized in PBS containing 0.5% Triton X-100 for 5 min at RT. Cells were then incubated with primary antibody for 2 hrs at RT, and detected with a secondary Alexa 488 or Alexa 545 conjugated goat anti-rabbit or anti-mouse IgG. Antibody dilutions and washes after incubations were performed in PBS. DNA was stained with DAPI (1 μg/ml) and coverslips were mounted in Shandon Immu-Mount medium (Thermo). Fluorescence microscopy was performed on a Nikon Eclipse T200 inverted microscope (Melville), equipped with a Hamamatsu Orca ER camera and a 200 W metal arc lamp (Prior Scientific, United Kingdom), with a 100×objective lens. Images were captured and analysed using Volocity 3.6.1 software (Improvision).

For live cell imaging, H2B–GFP HeLa cells were grown on 24-well glass bottomed plates (Scientific Laboratory Supplies) in selective media. Cells were transfected with siRNA or treated with nocodazole, then cells were imaged on a Leica AF6000 LX inverted microscope fitted with an environmental chamber set at 37℃ providing humidity and 5% CO_2. Leica LAS AF Lite software was used for image acquisition and analysis.

Flow cytometric analysis

Cells were pulsed with 10 μM BrdU (Sigma) for 20 min, then collected using trypsin. Pellets were washed with PBS, fixed in 70% ice-cold ethanol, and stored at −20℃ for up to 2 weeks. To denature DNA, fixed cells were resuspended in 2N HCl and incubated for 30 min at RT. After thoroughly washing with PBS, to remove any residual acid, cells were incubated with a mouse monoclonal anti-BrdU antibody diluted at a ratio of 1:50 in PBS-T (PBS containing 0.1% BSA and 0.2% Tween 20, pH 7.4) for 20 min at RT. Cells were then rinsed with PBS containing 0.2% Tween 20 and incubated with FITC-conjugated rabbit anti-mouse immunoglobulin diluted at a ratio of 1:10 in PBS-T. After a 20 min incubation at room temperature in the dark, cells were washed with PBS and stained with a propidium iodide solution (50 μg/ml) containing RNase A (25 μg/ml) for 30 min before flow cytometry was performed on a Becton Dickinson FACScalibur instrument. For staining with a phospho-histone H3 Ser10 antibody, the same protocol was followed, omitting the incubation with BrdU and the acid wash.

MTT growth assay

Cells were plated at a density of 1500 cells/well on 96-well plates, and the following day these were transfected with siRNA as indicated above. After the indicated times, MTT reagent was added to the cells at a final concentration of 1 mg/ml, and these were incubated at 37℃ for 3 hrs. The media was removed and replaced with 200 μl DMSO to solubilise the formazan product, and the absorbance of this product was assessed by quantifying optical density at 540 nm using a spectrophotometric microtitre plate reader.

Acknowledgements

HeLa cells expressing GFP–centrin-2 and H2B–GFP were kind gifts from Dr Fanni Gergely (Cambridge Research Institute, UK) and Prof. Peter Cook (Dunn School of Pathology, Oxford, UK), respectively. C-Nap1 antibody was a kind gift of Prof. Erich Nigg (University of Basel, Switzerland). pEGFP-C1-p50 dynamitin was a kind gift of Dr Andreas Merdes (University of Toulouse). We thank Dr Patrick Eyers and Dr Giancarlo Barone for insightful discussions

regarding this work and Prof. Mark Meuth, Dr Mark Petronczki and Dr Vincenzo Costanzo for critically reading the manuscript.

Funding

S.J.C. is funded by a Cancer Research UK (CR-UK) Senior Cancer Research Fellowship; and aspects of this work were also supported by Yorkshire Cancer Research (YCR). C.J.S., K.N.M., A.J.X.L., C.S., M.H., S.J.B. and S.J.C. are funded by CR-UK. R.D.D.B. and A.A.P. are funded by YCR.

Supplementary material available online at
http://jcs.biologists.org/lookup/suppl/doi:10.1242/jcs.104059/-/DC1

References

Andersen, J. S., Wilkinson, C. J., Mayor, T., Mortensen, P., Nigg, E. A. and Mann, M. (2003). Proteomic characterization of the human centrosome by protein correlation profiling. *Nature* **426**, 570-574.

Aoto, H., Tsuchida, J., Nishina, Y., Nishimune, Y., Asano, A. and Tajima, S. (1995). Isolation of a novel cDNA that encodes a protein localized to the pre-acrosome region of spermatids. *Eur. J. Biochem.* **234**, 8-15.

Aoto, H., Miyake, Y., Nakamura, M. and Tajima, S. (1997). Genomic organization of the mouse AZ1 gene that encodes the protein localized to preacrosomes of spermatids. *Genomics* **40**, 138-141.

Balczon, R., Bao, L. and Zimmer, W. E. (1994). PCM-1, A 228-kD centrosome autoantigen with a distinct cell cycle distribution. *J. Cell Biol.* **124**, 783-793.

Balczon, R., Bao, L., Zimmer, W. E., Brown, K., Zinkowski, R. P. and Brinkley, B. R. (1995). Dissociation of centrosome replication events from cycles of DNA synthesis and mitotic division in hydroxyurea-arrested Chinese hamster ovary cells. *J. Cell Biol.* **130**, 105-115.

Bonner, W. M., Redon, C. E., Dickey, J. S., Nakamura, A. J., Sedelnikova, O. A., Solier, S. and Pommier, Y. (2008). GammaH2AX and cancer. *Nat. Rev. Cancer* **8**, 957-967.

Coppieters, F., Lefever, S., Leroy, B. P. and De Baere, E. (2010). CEP290, a gene with many faces: mutation overview and presentation of CEP290base. *Hum. Mutat.* **31**, 1097-1108.

Dammermann, A. and Merdes, A. (2002). Assembly of centrosomal proteins and microtubule organization depends on PCM-1. *J. Cell Biol.* **159**, 255-266.

Dictenberg, J. B., Zimmerman, W., Sparks, C. A., Young, A., Vidair, C., Zheng, Y., Carrington, W., Fay, F. S. and Doxsey, S. J. (1998). Pericentrin and gamma-tubulin form a protein complex and are organized into a novel lattice at the centrosome. *J. Cell Biol.* **141**, 163-174.

Emdad, L., Sarkar, D., Su, Z. Z. and Fisher, P. B. (2005). Emerging roles of centrosomal amplification and genomic instability in cancer. *Front. Biosci.* **10**, 728-742.

Fukasawa, K. (2007). Oncogenes and tumour suppressors take on centrosomes. *Nat. Rev. Cancer* **7**, 911-924.

Ganem, N. J., Godinho, S. A. and Pellman, D. (2009). A mechanism linking extra centrosomes to chromosomal instability. *Nature* **460**, 278-282.

Gillingham, A. K. and Munro, S. (2000). The PACT domain, a conserved centrosomal targeting motif in the coiled-coil proteins AKAP450 and pericentrin. *EMBO Rep.* **1**, 524-529.

Gould, R. R. and Borisy, G. G. (1977). The pericentriolar material in Chinese hamster ovary cells nucleates microtubule formation. *J. Cell Biol.* **73**, 601-615.

Graser, S., Stierhof, Y. D., Lavoie, S. B., Gassner, O. S., Lamla, S., Le Clech, M. and Nigg, E. A. (2007). Cep164, a novel centriole appendage protein required for primary cilium formation. *J. Cell Biol.* **179**, 321-330.

Griffith, E., Walker, S., Martin, C. A., Vagnarelli, P., Stiff, T., Vernay, B., Al Sanna, N., Saggar, A., Hamel, B., Earnshaw, W. C. et al. (2008). Mutations in pericentrin cause Seckel syndrome with defective ATR-dependent DNA damage signaling. *Nat. Genet.* **40**, 232-236.

Janssen, A., van der Burg, M., Szuhai, K., Kops, G. J. and Medema, R. H. (2011). Chromosome segregation errors as a cause of DNA damage and structural chromosome aberrations. *Science* **333**, 1895-1898.

Kalay, E., Yigit, G., Aslan, Y., Brown, K. E., Pohl, E., Bicknell, L. S., Kayserili, H., Li, Y., Tuysuz, B., Nurnberg, G. et al. (2011). CEP152 is a genome maintenance protein disrupted in Seckel syndrome. *Nat. Genet* **43**, 23-26.

Kamiya, A., Tan, P. L., Kubo, K., Engelhard, C., Ishizuka, K., Kubo, A., Tsukita, S., Pulver, A. E., Nakajima, K., Cascella, N. G. et al. (2008). Recruitment of PCM1 to the centrosome by the cooperative action of DISC1 and BBS4: a candidate for psychiatric illnesses. *Arch. Gen. Psychiatry* **65**, 996.

Kim, K. and Rhee, K. (2011). The pericentriolar satellite protein CEP90 is crucial for integrity of the mitotic spindle pole. *J. Cell Sci.* **124**, 338-347.

Kim, J. C., Badano, J. L., Sibold, S., Esmail, M. A., Hill, J., Hoskins, B. E., Leitch, C. C., Venner, K., Ansley, S. J., Ross, A. J. et al. (2004). The Bardet-Biedl protein BBS4 targets cargo to the pericentriolar region and is required for microtubule anchoring and cell cycle progression. *Nat. Genet.* **36**, 462-470.

Kim, J., Choi, Y. L., Vallentin, A., Hunrichs, B. S., Hellerstein, M. K., Peehl, D. M. and Mochly-Rosen, D. (2008a). Centrosomal PKCbetaII and pericentrin are critical for human prostate cancer growth and angiogenesis. *Cancer Res.* **68**, 6831-6839.

Kim, J., Krishnaswami, S. R. and Gleeson, J. G. (2008b). CEP290 interacts with the centriolar satellite component PCM-1 and is required for Rab8 localization to the primary cilium. *Hum. Mol. Genet.* **17**, 3796-3805.

Kodani, A., Tonthat, V., Wu, B. and Sütterlin, C. (2010). Par6 alpha interacts with the dynactin subunit p150 Glued and is a critical regulator of centrosomal protein recruitment. *Mol. Biol. Cell* **21**, 3376-3385.

Krämer, A., Maier, B. and Bartek, J. (2011). Centrosome clustering and chromosomal (in)stability: a matter of life and death. *Mol. Oncol.* **5**, 324-335.

Lee, S. and Rhee, K. (2010). CEP215 is involved in the dynein-dependent accumulation of pericentriolar matrix proteins for spindle pole formation. *Cell Cycle* **9**, 775-784.

Li, Q., Hansen, D., Killilea, A., Joshi, H. C., Palazzo, R. E. and Balczon, R. (2001). Kendrin/pericentrin-B, a centrosome protein with homology to pericentrin that complexes with PCM-1. *J. Cell Sci.* **114**, 797-809.

Loncarek, J., Hergert, P., Magidson, V. and Khodjakov, A. (2008). Control of daughter centriole formation by the pericentriolar material. *Nat. Cell Biol.* **10**, 322-328.

Lopes, C. A., Prosser, S. L., Romio, L., Hirst, R. A., O'Callaghan, C., Woolf, A. S. and Fry, A. M. (2011). Centriolar satellites are assembly points for proteins implicated in human ciliopathies, including oral-facial-digital syndrome 1. *J. Cell Sci.* **124**, 600-612.

Ma, L. and Jarman, A. P. (2011). Dilatory is a Drosophila protein related to AZI1 (CEP131) that is located at the ciliary base and required for cilium formation. *J. Cell Sci.* **124**, 2622-2630.

Matsuoka, S., Ballif, B. A., Smogorzewska, A., McDonald, E. R., 3rd, Hurov, K. E., Luo, J., Bakalarski, C. E., Zhao, Z., Solimini, N., Lerenthal, Y. et al. (2007). ATM and ATR substrate analysis reveals extensive protein networks responsive to DNA damage. *Science* **316**, 1160-1166.

Meraldi, P., Lukas, J., Fry, A. M., Bartek, J. and Nigg, E. A. (1999). Centrosome duplication in mammalian somatic cells requires E2F and Cdk2-cyclin A. *Nat. Cell Biol.* **1**, 88-93.

Miyoshi, K., Asanuma, M., Miyazaki, I., Diaz-Corrales, F. J., Katayama, T., Tohyama, M. and Ogawa, N. (2004). DISC1 localizes to the centrosome by binding to kendrin. *Biochem. Biophys. Res. Commun.* **317**, 1195-1199.

Mogensen, M. M., Malik, A., Piel, M., Bouckson-Castaing, V. and Bornens, M. (2000). Microtubule minus-end anchorage at centrosomal and non-centrosomal sites: the role of ninein. *J. Cell Sci.* **113**, 3013-3023.

Moritz, M., Braunfeld, M. B., Sedat, J. W., Alberts, B. and Agard, D. A. (1995). Microtubule nucleation by gamma-tubulin-containing rings in the centrosome. *Nature* **378**, 638-640.

Nigg, E. A. (2006). Origins and consequences of centrosome aberrations in human cancers. *Int. J. Cancer* **119**, 2717-2723.

Nigg, E. A. and Raff, J. W. (2009). Centrioles, centrosomes, and cilia in health and disease. *Cell* **139**, 663-678.

Paulsen, R. D., Soni, D. V., Wollman, R., Hahn, A. T., Yee, M. C., Guan, A., Hesley, J. A., Miller, S. C., Cromwell, E. F., Solow-Cordero, D. E. et al. (2009). A genome-wide siRNA screen reveals diverse cellular processes and pathways that mediate genome stability. *Mol. Cell* **35**, 228-239.

Prosser, S. L., Straatman, K. R. and Fry, A. M. (2009). Molecular dissection of the centrosome overduplication pathway in S-phase-arrested cells. *Mol. Cell. Biol.* **29**, 1760-1773.

Silkworth, W. T., Nardi, I. K., Scholl, L. M. and Cimini, D. (2009). Multipolar spindle pole coalescence is a major source of kinetochore mis-attachment and chromosome mis-segregation in cancer cells. *PLoS ONE* **4**, e6564.

Sivasubramaniam, S., Sun, X., Pan, Y. R., Wang, S. and Lee, E. Y. (2008). Cep164 is a mediator protein required for the maintenance of genomic stability through modulation of MDC1, RPA, and CHK1. *Genes Dev.* **22**, 587-600.

Smith, E., Dejsuphong, D., Balestrini, A., Hampel, M., Lenz, C., Takeda, S., Vindigni, A. and Costanzo, V. (2009). An ATM- and ATR-dependent checkpoint inactivates spindle assembly by targeting CEP63. *Nat. Cell Biol.* **11**, 278-285.

Tynan, S. H., Purohit, A., Doxsey, S. J. and Vallee, R. B. (2000). Light intermediate chain 1 defines a functional subfraction of cytoplasmic dynein which binds to pericentrin. *J. Biol. Chem.* **275**, 32763-32768.

Wilkinson, C. J., Carl, M. and Harris, W. A. (2009). Cep70 and Cep131 contribute to ciliogenesis in zebrafish embryos. *BMC Cell Biol.* **10**, 17.

Young, A., Dictenberg, J. B., Purohit, A., Tuft, R. and Doxsey, S. J. (2000). Cytoplasmic dynein-mediated assembly of pericentrin and gamma tubulin onto centrosomes. *Mol. Biol. Cell* **11**, 2047-2056.

Journal of Cell Science